

Constraining the star formation and the assembly histories of normal and compact early-type galaxies at $1 < z < 2$.

P. Saracco^{1*}, M. Longhetti¹, A. Gargiulo¹

¹INAF - Osservatorio Astronomico di Brera, Via Brera 28, 20121 Milano, Italy

Accepted 2010 November 25. Received 2010 November 11; in original form 2010 August 11

ABSTRACT

We present a study based on a sample of 62 early-type galaxies (ETGs) at $0.9 < z_{spec} < 2$ aimed at constraining their past star formation and mass assembly histories. The sample is composed of normal ETGs having effective radii comparable to the mean radius of local ones and of compact ETGs having effective radii from two to six times smaller. We do not find evidence of a dependence of the compactness of ETGs on their stellar mass. The best fitting to their spectral energy distribution at known redshift has allowed us to constrain the epoch at which the stellar mass formed. We find that the stellar mass of normal ETGs formed at $z_{form} \lesssim 3$ while the stellar content of compact ETGs formed over a wider range of redshift ($2 < z_{form} < 10$) with a large fraction of them characterized by $z_{form} > 5$. Earlier stars, those formed at $z_{form} > 5$, are assembled in compact and more massive ($M_* > 10^{11} M_\odot$) ETGs while stars later formed ($z_{form} \lesssim 3$) or resulting from subsequent episodes of star formation are assembled both in compact and normal ETGs. Thus, the older the stellar population the higher the mass of the hosting galaxy but not vice versa. This suggests that the epoch of formation may play a role in the formation of massive ETGs rather than the mass itself. We show that the possible general scheme in which normal ETGs at $\langle z \rangle \simeq 1.5$ are descendants of compact spheroids assembled at higher redshift is not compatible with the current models. Indeed, we find that the number of dry mergers expected in a hierarchical model is almost two orders of magnitude lower than the one needed to enlarge a compact ETGs up to a normal-size ETG. Moreover, we do not find evidence supporting a dependence of the compactness of galaxies on their redshift of assembly, a dependence expected in the hypothesis that the compactness of a galaxy is due to the higher density of the Universe at earlier epochs. Finally, we propose a simple scheme of formation and assembly of the stellar mass of ETGs based on dissipative gas-rich merger which can qualitatively account for the co-existence of normal and compact ETGs observed at $\langle z \rangle \simeq 1.5$ in spite of the same stellar mass, the lack of normal ETGs with high z_{form} and the absence of correlation between compactness, stellar mass and formation redshift.

Key words: galaxies: evolution; galaxies: elliptical and lenticular, cD; galaxies: formation; galaxies: high redshift

1 INTRODUCTION

To understand how galaxies have formed and evolved it is fundamental to know which and how many of them were present in the Universe at different epochs. In the last years, many efforts have been devoted to trace the evolution of early-type galaxies back in time since they contain most of the present-day stars and baryons (e.g. Fukugita et al. 1998). After the first spectroscopic detection of early-type galaxies at $z \sim 1.5$ (Dunlop et al. 1996; Saracco et al. 2003; McCarthy et al. 2004; Cimatti et al. 2004; Glazebrook et al. 2004; Saracco et al. 2005), the attention was attracted by the small effective radius of many of them when compared to the mean ra-

dius of present-day early-types of comparable mass (Daddi et al. 2005; Trujillo et al. 2006; Longhetti et al. 2007). Since then, many works focused on the "small early-type galaxies problem" corroborating the idea that in the past early-type galaxies were smaller at fixed mass, hence denser (McGrath et al. 2008; Cimatti et al. 2008; Buitrago et al. 2008; van Dokkum et al. 2008; Damjanov et al. 2009; Muzzin et al. 2009; Cassata et al. 2010; Carrasco et al. 2010). As a consequence of this, ETGs must have increased their radius across the time to reconcile with the present-day early-types. However, evidence of a significant number of normal ETGs at $z \sim 1.5$ following the local scaling relations has been accumulated in the last couple of years suggesting that at least not all the high- z early-types were more compact (Saracco et al. 2009; Mancini et al. 2010) and that, consequently, not all the high- z ETGs undergo size evo-

* E-mail: paolo.saracco@brera.inaf.it

lution. The first measurements of velocity dispersion of a few of “normal-size” high- z ETGs confirmed that they are similar to typical local ones also from the dynamic point of view (Cenarro et al. 2009; Cappellari et al. 2009; Onodera et al. 2010). Concurrently, evidence of the presence of a significant fraction of compact ETGs in the local Universe similar to the high- z ones came out (e.g. Trujillo et al. 2009; Valentinuzzi et al. 2010a; 2010b) casting the first doubts about the size evolution scenario. The question naturally arising from these new pieces of evidence is whether compact ETGs were so much more numerous at earlier epochs to require their effective radius evolution. Recently, evidence that the number density of compact ETGs at $\langle z \rangle \simeq 1.5$ was not significantly higher than the number density of compact ETGs seen in local cluster of galaxies has come out (Saracco, Longhetti & Gargiulo 2010). This evidence conflicts with the hypothesized effective radius evolution of high- z ETGs while shows that among them there are the progenitors of the compact ETGs seen in local clusters of galaxies and that they were as we see them today already 9-10 Gyr ago as confirmed by recent studies on high- z cluster galaxies (e.g. Strazzullo et al. 2010). Moreover, at $z \sim 1.5$ a majority of normal ETGs co-exist with compact early-types from ~ 2 to ~ 6 times smaller in spite of the same mass and redshift. Actually, this picture is not different at least qualitatively from what is observed in the local universe: most of the ETGs lie on a well defined scaling relation and a minor fraction of them (e.g. ~ 20 -40 per cent in cluster of galaxies, Valentinuzzi et al. 2010a; 2010b) are significantly denser than the others. Thus, ETGs appear a composite population from $z = 0$ up to at least $z \sim 1.5 - 2$. To corroborate this view is the recent study conducted by Gargiulo et al. (2010) who show that at $1 < z < 2$ ETGs with negative color gradient (redder toward the center) co-exist with ETGs characterized by positive color gradient (bluer toward the center). Consequently, this non homogeneity of the population of ETGs must originate at an earlier epoch ($z > 2$) when they have been assembled. The relevant question is which formation scenario and early physical conditions can account for the observed different properties of ETGs. In this paper we try to constrain these issues by probing the past history of a large number of ETGs at $0.9 < z_{spec} < 2$. In Sec. 2 we describe the data set we used in this analysis. In Sec. 3 we describe our analysis and we present the results. In Sec. 4 we use the results obtained to derive some constraints on the spheroids formation at very early epochs. Finally, in Sec. 5, we summarize the results and present the conclusions. Throughout this paper we use a standard cosmology with $H_0 = 70 \text{ Km s}^{-1} \text{ Mpc}^{-1}$, $\Omega_m = 0.3$ and $\Omega_\Lambda = 0.7$. All the magnitudes are in the Vega system, unless otherwise specified.

2 THE DATA SET

The sample of ETGs we used in our analysis is composed of 62 ETGs in the spectroscopic redshift range $0.9 < z_{spec} < 2$ and with magnitudes in the range $17 < K < 20.5$. The whole sample is covered by HST observations at spatial resolution of about 0.8 kpc (FWHM ~ 0.1 arcsec) at the redshift of the galaxies. Out of the 62 ETGs, 28 are covered by observations with the Near Infrared Camera and Multi Object Spectrograph (NICMOS sample hereafter) in the F160W filter and 34 are covered by observations with the Advanced Camera for Surveys (ACS sample hereafter). The NICMOS sample is a compilation of early-type galaxies at $1.2 < z_{spec} < 1.85$ which combines proprietary data (Longhetti et al. 2007) with those from other surveys for a total of 32 ETGs in its original form (Saracco et al. 2009). Here, we removed 4 galax-

ies due to the poor fitting to their profile obtained on the NIC3 images. The wavelength coverage is composed of 10 photometric bands (from 0.4 μm to 3.6 μm) for most of the sample. The ACS sample is a complete sample of ETGs we selected at $K \leq 20.2$ (Saracco et al. 2010) on the southern field of the Great Observatories Origins Deep Survey (GOODS; Giavalisco et al. 2004) with redshift $0.9 < z_{spec} < 1.92$. The wavelength coverage of the ACS sample is composed of 14 photometric bands extending from 0.3 μm to 8.0 μm . The complete ACS sample will be presented in a forthcoming paper (Saracco et al. in preparation).

The effective radii of the galaxies were derived by fitting a Sérsic profile to the observed light profile in the HST NICMOS-F160W and ACS-F850LP images. Stellar masses \mathcal{M}_* and ages of the stellar populations were derived by fitting the red-shifted templates to the observed spectral energy distribution of the galaxy. We used the last release of the stellar population synthesis models of Charlot & Bruzual with Chabrier initial mass function (IMF, Chabrier 2003), four exponentially declining star formation histories (SFHs) with e-folding time $\tau = [0.1, 0.3, 0.4, 0.6]$ Gyr and metallicity $0.4 Z_\odot$, Z_\odot and $2 Z_\odot$. The profile fitting and the SED fitting of galaxies are described in detail in the previous papers (Saracco et al. 2009; 2010). In Tab. 1 we report the main properties and the best fitting parameters for the 62 ETGs considered in the present analysis.

3 PROBING THE BUILD-UP OF NORMAL AND COMPACT EARLY-TYPE GALAXIES

Fig. 1 shows the relation between the effective radius R_e [kpc] and the stellar mass \mathcal{M}_* [M_\odot] of the 62 ETGs considered in the present work (filled symbols). The different colors used in the upper panel mark the different redshift interval which the galaxies belong to: blue corresponds to $0.9 < z_1 < 1.2$, cyan to $1.2 < z_2 < 1.5$ and magenta to $1.5 < z_3 < 2$. The size-mass (SM) relation found by Shen et al. (2003) for the local population of ETGs is also shown (solid line). The fraction of normal ETGs, which we define as those lying within one sigma from the local relation (taking also into account the errors on size measurements), is ~ 50 per cent (29 out of 62 ETGs; filled triangles), slightly smaller than the fraction (62 per cent) derived from the complete ACS sample (Saracco et al. 2010). We are not inclined to ascribe the higher fraction of compact ETGs in the NICMOS sample to a systematic difference of the size of galaxies when observed at different wavelengths since no evidence in favour of this effect is emerging (e.g. McGrath et al. 2008; Cassata et al. 2010). We are rather inclined to ascribe this difference to the fact that the NICMOS sample collects ETGs pre-selected on the basis of their red colors (e.g. R-K > 5), i.e. their old age. Since old ETGs are smaller for fixed mass and more massive for fixed radius (e.g. Bernardi et al. 2008; Valentinuzzi et al. 2010) NICMOS sample is consequently biased toward compact ETGs. We verified this by using the complete ACS sample, unbiased with respect to any color selection. We have selected galaxies from this sample at different F606W-K colors (close to R-K color) and we have count the fraction of compact ETGs, which we define as those falling more than one sigma below the local size-mass relation, at different color cuts. The result is shown in Fig. 2 where the fraction of compact ETGs is shown as a function of F606W-K color cuts. It is evident that the fraction of compact ETGs increases systematically toward redder color cuts showing the strong selection effect affecting the NICMOS sample and all those ETG samples constructed using this kind of color pre-selection. For clarity, in

Table 1. Sample of 62 ETGs. In the left panel 28 ETGs out of the 32 ETGs of the NICMOS sample (Saracco et al. 2009) are listed. Four galaxies have not been considered in the present analysis because of the very poor fitting to their profile on the HST-NIC3 images (0.2 arcsec/pix). For each galaxy of the two sub-samples (NICMOS and ACS) we report the total apparent magnitude (F160W and F850LP) measured on the HST images used to perform the profile fitting, the total magnitude of the best fitting profile derived by `galfit` (F160W_{fit} and F850LP_{fit}), the effective radius R_e , the degree of compactness $C = R_e/R_{e,z=0}$ (see §3), the age and the stellar mass provided by the SED fitting (see §2). The errors on the measured magnitude F160W are in the range 0.04-0.1 mag while those on the F850LP are in the range 0.01-0.05 mag. The typical error on the best fitting profile magnitude is 0.02 mag.

NICMOS sample								ACS sample							
ID	z_{spec}	F160W [mag]	F160W _{fit} [mag]	R_e [kpc]	C	Age [Gyr]	$\log(M_*)$ [M_\odot]	ID	z_{spec}	F850LP [mag]	F850LP _{fit} [mag]	R_e [kpc]	C	Age [Gyr]	$\log(M_*)$ [M_\odot]
S2_109	1.22	17.75	17.47	4.4±0.2	0.34	3.5	11.88	01	1.921	23.96	23.84	0.5±0.1	0.20	1.0	10.56
S7_254	1.22	19.58	19.46	2.3±0.2	0.26	4.5	11.59	02	1.609	23.52	23.31	1.1±0.1	0.25	3.2	10.99
S2_357	1.34	19.04	18.72	2.8±0.2	0.28	4.2	11.69	03	1.609	23.03	22.75	1.6±0.1	0.27	3.5	11.17
S2_389	1.40	20.08	19.79	2.1±0.3	0.36	3.5	11.26	04	1.610	23.53	23.33	0.8±0.1	0.29	1.0	10.57
S2_511	1.40	19.37	19.15	2.1±0.2	0.54	1.0	10.95	05	1.123	21.39	21.08	1.4±0.1	0.36	2.4	10.81
S2_142	1.43	19.00	18.65	3.1±0.2	0.38	3.5	11.61	06	1.032	22.27	22.08	0.4±0.1	0.32	1.0	10.00
S7_45	1.45	18.59	18.83	4.7±0.3	0.77	1.0	11.30	07	1.612	24.22	23.91	2.1±0.3	0.42	3.0	10.99
S2_633	1.45	19.32	19.00	2.6±0.2	0.37	2.6	11.40	08	1.610	23.78	23.67	0.8±0.1	0.39	0.9	10.40
S2_443	1.70	19.69	19.44	3.4±0.3	0.41	3.2	11.53	09	1.044	21.32	20.98	1.4±0.1	0.46	2.0	10.62
S2_527	1.35	19.80	19.50	1.7±0.3	0.39	2.3	11.04	10	1.215	21.67	21.55	1.2±0.1	0.47	1.0	10.60
S-5592	1.623	20.40	20.30	1.4±0.3	0.30	0.9	10.48	11	1.614	23.30	22.92	2.0±0.2	0.54	1.7	10.75
S-5869	1.510	19.64	19.53	2.8±0.3	0.35	1.2	10.60	12	0.964	20.05	19.98	3.6±0.1	0.56	3.0	11.31
S-6072	1.576	21.06	20.96	1.4±0.3	0.45	1.4	10.48	13	1.910	23.33	22.97	2.9±0.2	0.57	0.9	11.00
S-8025	1.397	19.94	19.87	2.4±0.3	0.52	3.7	10.70	14	1.096	20.32	20.20	4.2±0.4	0.60	2.7	11.36
S-8895	1.646	19.44	19.20	3.9±0.3	0.49	0.8	10.85	15	1.096	21.46	21.46	2.4±0.3	0.61	3.2	10.96
S-4367	1.725	20.75	20.61	2.5±0.3	0.88	0.9	10.60	16	1.604	23.87	23.72	1.2±0.1	0.58	1.1	10.38
S-5005	1.845	20.59	20.46	2.1±0.3	0.67	0.9	10.60	17	1.297	22.35	22.27	2.0±0.2	0.64	2.3	10.74
S-7543	1.801	19.70	19.64	3.3±0.3	0.79	1.0	10.95	18	1.097	22.44	22.15	1.2±0.1	0.61	1.9	10.33
S-0189	1.490	19.27	19.19	3.2±0.3	0.40	3.5	11.26	19	1.125	21.78	21.48	2.1±0.1	0.66	2.1	10.66
S-1983	1.488	20.02	20.03	1.5±0.3	0.32	3.7	11.00	20	1.039	21.28	20.97	2.4±0.1	0.68	2.5	10.74
C_237	1.271	20.38	20.14	3.0±0.6	1.40	3.5	10.48	21	1.022	20.84	20.41	3.8±0.1	0.74	2.7	11.00
C_65	1.263	18.71	18.85	3.3±0.3	0.52	4.2	11.32	22	1.019	22.92	22.72	0.6±0.1	0.65	1.1	9.77
C_142	1.277	19.67	19.63	1.6±0.4	0.38	4.2	11.00	23	1.089	20.67	20.34	3.2±0.1	0.78	0.8	10.86
C_135	1.276	19.37	19.33	4.7±0.4	1.19	4.3	10.95	24	0.980	20.17	19.83	3.7±0.1	0.80	1.6	10.94
H_1031	1.015	19.57	19.37	2.1±0.2	1.24	1.1	10.30	25	0.964	20.12	19.69	5.7±0.1	0.95	2.6	11.11
H_1523	1.050	18.00	17.67	4.8±0.8	0.79	2.0	11.32	26	1.415	23.45	23.26	2.1±0.2	0.87	1.1	10.48
H_731	1.755	20.24	20.20	4.6±0.8	1.84	1.4	10.60	27	1.221	22.92	22.55	2.2±0.2	0.91	2.4	10.43
W091	1.55	19.64	19.77	1.6±0.2	0.51	2.4	10.78	28	1.041	21.59	21.19	2.8±0.1	0.97	1.9	10.55
—	—	—	—	—	—	—	—	29	1.188	22.78	22.45	2.4±0.2	1.01	2.5	10.44
—	—	—	—	—	—	—	—	30	1.222	22.27	22.06	2.4±0.1	1.10	1.1	10.42
—	—	—	—	—	—	—	—	31	1.135	20.53	20.28	9.3±0.9	1.30	2.6	11.32
—	—	—	—	—	—	—	—	32	1.170	22.31	21.87	3.5±0.2	1.34	2.4	10.46
—	—	—	—	—	—	—	—	33	1.330	21.95	21.31	7.9±0.7	1.48	1.8	10.93
—	—	—	—	—	—	—	—	34	0.984	21.29	20.73	4.4±0.4	1.43	1.7	10.54

Fig. 3 the same relations shown in Fig. 1 are presented using different symbols (and colors) for the galaxies belonging to the two sub-samples: starred (magenta) symbols represent the ETGs of the NICMOS sample while open (cyan) circles those belonging to the ACS sample. It is evident the different distribution of the NICMOS sample with respect to the ACS sample in the size-mass plane. Most importantly, it is evident the larger fraction of compact ETGs in the NICMOS sample, particularly at large stellar masses ($M_* \gtrsim 10^{11}$) where all the NICMOS ETGs are compact. This is the reason why, in Fig. 1 at masses $M_* > 3 \times 10^{11} M_\odot$, a range populated only by galaxies belonging to the NICMOS sample (see Fig. 3) there are only compact ETGs. In spite of this, Fig. 1 (lower panel) shows that the compactness of a galaxy, defined as the ratio between its effective radius R_e and the effective radius $R_{e,z=0}$ of an equal mass galaxy at $z = 0$ derived from the local SM relation, does not show any trend with mass. This evidence conflicts with the hypothesis of a mass-dependent size evolution of ETGs, hypothesis suggested by many authors. For instance, it has been suggested that only high-

mass ETGs undergo size evolution (e.g. Newman et al. 2010) or that they undergo the most rapid evolution (e.g. Ryan et al. 2010) being them on average smaller than their local counterparts. At the same time, other authors have suggested at odd with this that only low-mass ETGs undergo size evolution to match the apparent lack of compact low-mass ETGs in the local Universe (e.g. van der Wel et al. 2009). Actually, we find that normal and compact ETGs co-exist for large intervals of effective radius ($0.4 \text{ kpc} < R_e < 8 \text{ kpc}$) and of the stellar mass ($10^{10} M_\odot < M_* \lesssim 10^{12} M_\odot$) as already found on a smaller but complete sample of ETGs (Saracco et al. 2010).

In Fig. 4 (left-hand panels) the compactness $R_e/R_{e,z=0}$ (upper panel), the stellar mass M_* (middle panel) and the effective stellar mass density $\rho_e = 0.5 M_* / (\frac{4}{3} \pi R_e^3)$ (we assumed that M/L is radially constant; lower panel) for the 62 ETGs of our sample are shown as a function of their redshift. It is evident the co-existence of normal-size ETGs ($R_e \approx R_{e,z=0}$ and $10^7 < \rho_e < 10^9 M_\odot \text{ kpc}^{-3}$) with ETGs of the same mass but with $R_e \approx [0.5 - 0.2] \times R_{e,z=0}$, that is 10-100 times denser ($\rho_e > 10^9 M_\odot \text{ kpc}^{-3}$). The origin of this extremely

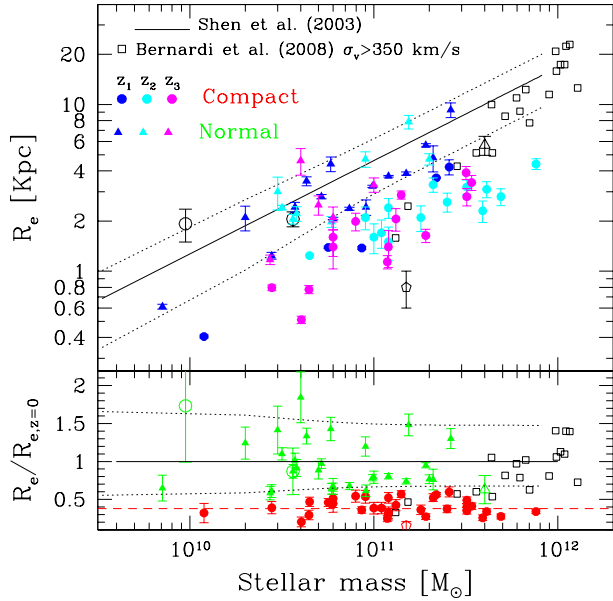


Figure 1. Upper panel - Effective radius R_e versus stellar mass for our sample of 62 ETGs. The solid line is the local Size-Mass relation (Shen et al. 2003). Normal ETGs lying within 1 sigma (dotted lines) from the local relation, are marked by filled triangles. Compact early-types diverging more than 1σ from the local relation (including errors on size measurements) are marked by filled circles. Filled symbols are color-coded according to the redshift of the galaxy. In particular, the three different colors blue, cyan and magenta mark the three redshift intervals $0.9 < z_1 < 1.2$, $1.2 < z_2 < 1.5$ and $1.5 < z_3 < 2$ respectively. The two open circles represent the ETGs with velocity dispersion measured by Cappellari et al. (2009) one of which belonging to our ACS sample, the open pentagon is the one measured by van Dokkum et al. (2009) and the open triangle is the one by Onodera et al. (2010). The open squares represents the 29 early-types selected by Bernardi et al. (2008) at $z < 0.1$ with velocity dispersion $\sigma_v > 350$ km/s. Lower panel - The compactness, defined as the ratio between the effective radius R_e of the galaxy and the effective radius $R_{e,z=0}$ of an equal mass galaxy at $z = 0$ as derived by the local S-M relation, is plotted as a function of the stellar mass. Symbols are as in the upper panel. In this case normal ETGs are marked by green filled triangles while compact ETGs by red filled circles for clarity. The (red) dashed line represents the mean compactness value of compact ETGs $R_e/R_{e,z=0} \approx 0.38$.

large spread in the properties of ETGs at $0.9 < z < 2$ necessarily originates before $z \sim 2$, during their assembly. Therefore, we searched for differences in their past history to sketch a possible scenario.

3.1 Constraining the formation of the stellar mass

There is not direct gauge of how and when the stellar mass has been assembled to form and to shape an early-type galaxy. However, the age of the stellar population fixes at least the epoch at which the stellar mass formed even if, according to the present models of galaxy formation, mass assembly and epoch of star formation are not necessarily concurrent (e.g. De Lucia et al. 2006). We derived for each galaxy the formation redshift $z_{form} = z(t_{form})$, where $t_{form} = age_{Univ}(z_{spec}) - age_{star}(z_{spec})$ is the epoch at which the bulk of the stellar mass was already formed, $age_{Univ}(z_{spec})$ is the age of the universe at the redshift of the galaxy and $age_{star}(z_{spec})$ is the age of the stellar population provided by the best fitting model to the observed SED of the galaxy at its redshift. In the right-hand panels

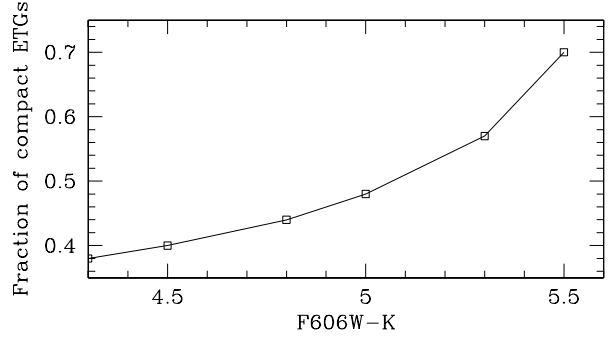


Figure 2. Fraction of compact ETGs (falling below one sigma from the local SM relation) in the complete ACS sample as a function of color F606W-K. It is evident the increasing fraction of compact ETGs at increasing red color.

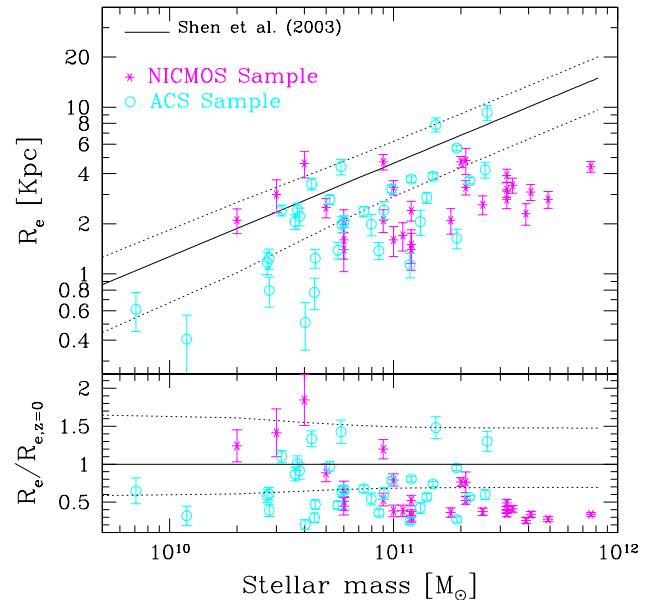


Figure 3. Same as Fig. 1. In this case the effective radius R_e (upper panel) and the compactness (lower panel) of galaxies are plotted versus their stellar mass using different symbols according to the sample they belong to: starred (magenta) symbols mark the ETGs of the NICMOS sample while open (cyan) circles the ETGs of the ACS sample. It is evident the larger fraction of compact ETGs in the NICMOS sample, particularly at $M_* \gtrsim 10^{11}$ where all the ETGs are compact.

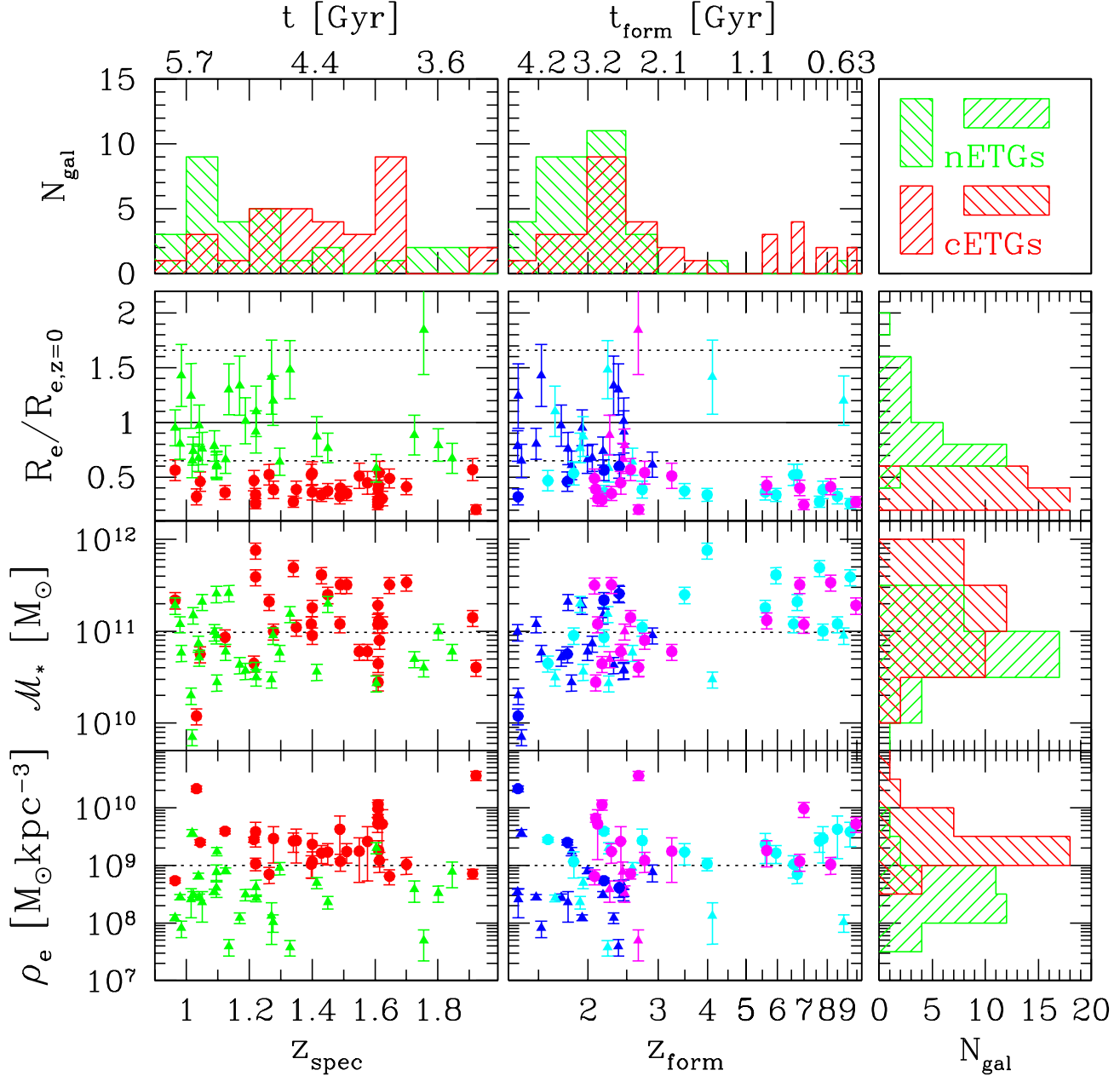


Figure 4. The compactness $R_e/R_{e,z=0}$ (upper panels), the stellar mass M_* (middle panels) and the effective stellar mass density $\rho_e = 0.5M_*/(\frac{4}{3}\pi R_e^3)$ (lower panels) of a galaxy are shown as a function of redshift z_{spec} (left-hand panels) and of the formation redshift z_{form} (right-hand panels) for the whole sample of 62 ETGs at $0.9 < z_{spec} < 2$. Triangles and circles mark normal and compact ETGs respectively in all the panels. The histograms at the top of the figure represent the distributions of redshift (left-hand) and of formation redshift (right-hand) for normal ETGs (nETGs, green shaded) and for compact ETGs (cETGs, red shaded). On the upper x-axis the age of the universe at the different redshift z_{spec} and at the different formation redshift z_{form} is shown. The histograms at the right-hand side of the figure represent the distributions of the compactness (upper panel), of the stellar mass (middle panel) and of the effective stellar mass density (lower panel) for normal and compact ETGs. In the left-hand panels normal and compact are identified by green and red colors respectively. In the right-hand panels, showing quantities as a function of z_{form} , galaxies are marked with different colors (blue, cyan and magenta) according to the redshift range they belong to ($0.9 < z_1 < 1.2$, $1.2 < z_2 < 1.5$ and $1.5 < z_3 < 2$ respectively), as in Fig. 1. The solid line in the compactness vs z_{spec} and z_{form} panels represents the relation $R_e/R_{e,z=0} = 1$ while the dotted lines are the 1 sigma dispersion of the local SM relation measured at $10^{11} M_\odot$. In the middle and in the lower panels the dotted lines at $M_* = 10^{11} M_\odot$ and at $\rho_e = 10^9 M_\odot \text{ kpc}^{-3}$ mark the median values.

of Fig. 4 the compactness, the stellar mass and the effective stellar mass density are shown as a function of their formation redshift z_{form} . The different colors blue, cyan and magenta mark the different spectroscopic redshift ranges $0.9-1.2$, $1.2-1.5$ and $1.5-2$ which the galaxies belong to. When the redshift (left-hand panels) is con-

sidered normal and compact do not show any convincing trend with z_{spec} . Their redshift distributions, shown at the top of Fig. 4, peak at different redshift, higher for compact ETGs and lower for normal ETGs even if they extend over the same redshift range. The peak at $z_{spec} \approx 1.6$ of compact ETGs is due to the high-density sheet-like

structure present in the GOODS-South field (Kurk et al. 2009) containing 5 compact ETGs. The two distributions are different at ~ 95 per cent confidence level being $P_{KS} \approx 5 \times 10^{-2}$ the probability of the two samples Kolmogorov-Smirnov (KS) test. The increasing fraction of compact ETGs with redshift (from 29 per cent (6/21) at $z_{spec} = 0.9 - 1.2$ to 64 per cent (14/22) at $z_{spec} = 1.2 - 1.5$) also visible in Fig. 1 when the whole sample of 62 ETGs is considered, is actually due to the high number of compact ETGs present in the NICMOS sample. Indeed, if we consider the complete ACS sample, the fraction of compact ETGs in the same redshift ranges are 21 per cent (4/19) and 17 per cent (1/6) respectively. However, we have to note that in the highest redshift bin $z_{spec} = 1.5 - 2$ the fraction of compact ETGs increases to 50 per cent (2/4, not considering the overdensity) even if the very low statistics does not make significant this difference. When z_{form} is considered almost all (27 out of 29) the normal ETGs are segregated at $z_{form} < 3$, while compact ETGs are distributed over a much wider interval with half of them (16 out of 33) at $z_{form} > 3$ and 40 per cent, 13 out of 33, at $z_{form} > 5$ (right-hand diagrams). The distributions of the formation redshift of compact and normal ETGs (histogram at the top of Fig. 4) differ at 99.95 per cent confidence level ($P_{KS} \approx 5 \times 10^{-4}$). The difference between the two z_{form} distributions is represented by the large number of compact ETGs with $z_{form} > 5$ (and $z_{spec} < 1.5$), an interval actually populated only by them. Also, Fig. 4 (middle-right panel) shows that they are massive ($M_* > 10^{11} M_\odot$) and, consequently, highly dense ($\rho_e \gtrsim 10^9 M_\odot \text{ kpc}^{-3}$; lower-right panel). On the contrary, at $z_{form} < 3$ there are both normal and compact galaxies independently of stellar mass and mass density. In this connection, we note that the distributions of the stellar mass of normal and compact ETGs shown at the right-hand side of Fig. 4 differ at 99 per cent confidence level ($P_{KS} \approx 8 \times 10^{-3}$) due to the high-mass tail ($M_* > 3 \times 10^{11} M_\odot$) of compact ETGs. We point out that the distributions of the compactness $R_e/R_{e,z=0}$ and of the effective stellar mass density ρ_e of normal and compact ETGs differ by definition of normal and compact galaxy. Strictly speaking, Fig. 4 shows that earlier stars, those characterized by $z_{form} > 5$ are preferentially assembled in compact, more massive and hence denser ETGs while stars later formed ($z_{form} < 3$), or possibly resulting from subsequent episodes of star formation, are assembled both in compact and in normal ETGs independently of their mass. It is worth noting that this behaviour only partially agrees with the "downsizing" pattern (Cowie et al. 1996; Gavazzi et al. 2002) where the higher the mass the older the stellar population and hence the higher the formation redshift. Indeed, Fig. 4 shows that the older the stellar population the higher the mass, but not vice versa. Indeed, we see ETGs with $z_{form} < 3$ with masses as large as those with $z_{form} > 5$. Thus, it seems that the epoch of formation may play a role in the formation of massive ETGs rather than the mass itself. Given the rapid decline ($0.1 \leq \tau \leq 0.3$ Gyr) of the SFHs ($\tau^{-1} e^{-t/\tau}$) of our ETGs it follows that the bulk of the stellar mass is produced within 1 Gyr. For those compact ETGs with $z_{form} > 5$ this has taken place $\approx 12 - 12.5$ Gyr ago, while for those with $z_{form} < 3$ at later times or possibly through subsequent episodes. Actually, these behaviours are qualitatively similar to those found in local ETGs. For instance, Thomas et al. (2005; 2010) studying a local sample of early-type galaxies, showed that the peak of the star formation efficiency occurred 12 Gyr ago for the most massive ETGs and that the higher the mass the shorter and more efficient the burst. Gargiulo et al. (2009), studying the fundamental plane (FP) of local ETGs find that for a given mass galaxies more compact than expected from the FP relation have experienced their last burst of star formation at earlier epochs. We tried to put in the context of galaxy formation

models our results on the star formation histories of high- z ETGs in order to constrain their possible assembly history.

3.2 Constraining the assembly of the stellar mass

In the current paradigm of galaxy formation the build-up of ETGs follows a hierarchical merging scheme along which mergers between sub-units can be dissipative (gas-rich) or dissipation-less ("dry"). This scheme has to account for the co-existence at $1 < z < 2$ of ETGs already shaped and grown in mass ($10^{10} M_\odot < M_* < 10^{12} M_\odot$), with very different stellar mass densities ($10^8 \lesssim \rho_e \lesssim 10^{10} M_\odot \text{ kpc}^{-3}$) and with stellar populations apparently formed at different epochs ($1.5 - 2 < z_{form} < 10$). Given the redshift of our ETGs ($1 < z < 2$) it follows that the above non homogeneity must be realized at $z > 2$. This leads to 3-4 Gyr the time at disposal to realize the above properties.

Let us first consider compact ETGs at $z \gtrsim 1.5$. They should be a natural consequence of the dissipative spheroid formation. Indeed, gas-rich merger is the known mechanism able to build compact ETGs on condition that the starburst resulting from the central dissipative gas collapse produces a large fraction ($\gtrsim 50$ per cent) of the stars of the remnant (e.g. Springel & Hernquist 2005; Khochfar & Silk 2006a, 2006b; Naab et al. 2007, 2009; Ciotti et al. 2007; Hopkins et al. 2008). Actually, the higher the fraction of stars formed in the merger the smaller the remnant at fixed mass (e.g. Khochfar & Silk 2006a). A typical time scale of merging in case of nearly equal mass merging galaxies is $\tau_{merge} \approx \tau_{dyn} \approx 1.5$ Gyr (e.g. Boylan-Kolchin et al. 2008), where τ_{dyn} is the dynamical time. Naab et al. (2007) found that their simulated galaxies start forming galaxies at $z \approx 3 - 5$ concurrently with the intense phase of merging and that after about 1.5-2 Gyr ($z \approx 2.5 - 2$) they were assembled almost 80 per cent of their final stellar mass (see also Sommer-Larsen and Toft 2010). Thus, for a compact ETG the assembly of the stellar mass can be considered nearly concurrent with its formation, that is $z_{assembly} \approx z_{form}$. Stated this, the constraints on the formation of the stellar mass of compact ETGs derived above (§3.1) suggest two possible interpretations for their assembly. The first one is that if the z_{form} values are reliable for all the compact ETGs then, given the formation redshift $2 \lesssim z_{form} < 10$ (see Fig. 4), it follows that the assembly of compact ETGs has taken place over the range $2 < z_{assembly} < 10$. This implies that the physical conditions able to produce compact ETGs (dissipative gas-rich merger) occur independently of redshift, at least in the above redshift range. According to this interpretation, ~ 40 per cent of the compact ETGs in our sample, those with $z_{form} > 5$, assembled at $z_{assembly} \gtrsim 5$. Perhaps, we should more properly say that the first ETGs assembled at $z_{assembly} \gtrsim 5$, were compact and more massive than $10^{11} M_\odot$ (right-hand panels of Fig. 4). The other possibility is that minor bursts of star formation occurred later have made some of the compact ETGs looking younger lowering the z_{form} , that is the low z_{form} values (e.g. $z_{form} < 3 - 5$) are not reliable. It is important to point out that in a dissipative merger where a large fraction of stars necessarily results from the central starburst ignited by the merger itself, it is easy to lower the *mean* age of the resulting stellar population and hence the formation redshift hypothesizing one or more small starburst episodes occurred later while it is difficult to realize the opposite condition. The spectra of our galaxies do not show signs of ongoing star formation and we do not find any systematic difference in the SED fitting of $z_{form} > 5$ and $z_{form} < 3$ compact ETGs. We also performed the fitting by neglecting in turn the UV rest-frame data of the SED dominated by the youngest stars and the near-IR rest-frame data dominated by the oldest stars without obtaining dif-

ferences in the best fitting templates. However, this is not sufficient to exclude the small starbursts hypothesis since even a single burst adding a few per cent of young stars can affect the mean age of the stellar population of a galaxy (e.g. Longhetti et al. 2005; Serra & Trager 2007; Thomas et al. 2010). Thus, in the hypothesis of one or more small starburst(s) occurred later, not only those with $z_{form} > 5$ but also the other compact ETGs could have been assembled at $z_{assembly} \gtrsim 5$ according to the reasonable hypothesis that the occurrence of dissipative mergers is dependent on redshift, much more probable at high- z given the larger fraction of gas at disposal (e.g. de Lucia et al. 2006). To summarize, our results suggest that in a dissipative merging scheme the assembly of compact ETGs has taken place at high- z ($z_{assembly} > 5$) for most of them or for a large fraction (40% in the present sample) of them at least. This latter case requires that dissipative gas-rich merger can occur efficiently over a wide redshift range, at least at $z > 1$.

Let us now consider normal ETGs at $z < z_{form} \approx 1.5$. We notice that normal ETGs span nearly the same mass range of compact ETGs but their stellar population seems to be formed more recently ($z_{form} < 3$). The main hypothesis to probe is whether they are descendants of the compact/dense ETGs assembled at high- z . Actually, we investigated the general scheme in which all the ETGs assembled at high- z as compact/dense spheroids and a fraction of them grow in size by adding a low stellar mass density envelope through subsequent gas-poor minor mergers at later times (e.g. Hopkins et al. 2009; Naab et al. 2009; Bezanson et al. 2009). Given the constraints on the redshift of assembly of compact ETGs derived above ($z_{assembly} > 5$) and the redshift range covered by our sample ($0.9 < z < 2$) it follows that the possible subsequent gas-poor minor mergers should occur at $1.5 - 2 \lesssim z < 5$, that is a fraction of the compact spheroids formed at $z > 5$ should increase their size from 2 to 6 times in about 2.5 Gyr. The above fraction corresponds to a number density not lower than $(5.5 \pm 3) \times 10^{-5} \text{ Mpc}^{-3}$, which is the number density of normal ETGs observed at $\langle z \rangle = 1.5$ with masses $[0.1 - 4] \times 10^{11} \text{ M}_\odot$ (Saracco et al. 2010). It is worth noting that in the case of minor mergers the typical time scales are $\tau_{merge} > 3 - 4 \text{ Gyr}$ (e.g. Boylan-Kolchin et al. 2008), thus larger than the 2.5 Gyr at disposal. Simulations suggest that the effective radius increases with merging as $R_e \propto M^\alpha$ with $0.6 < \alpha < 1.3$ (e.g. Boylan-Kolchin et al. 2006; Khochfar & Silk 2006a, 2006b; Ciotti et al. 2007). However, recently, it has been shown that the accretion of a low stellar mass density envelope through dry minor merging can be even more efficient in enlarging the size (Naab et al. 2009). Thus, for our calculations we considered the extreme value $\alpha = 1.5$. In this extremely favourable case a galaxy should at least double its mass to increase its effective radius by a factor 3. Assuming a maximum mass ratio 1:3 for the merging galaxies involved in minor mergers, at least 3 minor mergers are needed to double the mass of a compact ETG in 2.5 Gyr. We used the merger rate calculator described by Hopkins et al. (2010b) to derive the number of minor mergers which a galaxy in the mass range $[0.1 - 4] \times 10^{11} \text{ M}_\odot$ can experience at $1.5 - 2 \lesssim z < 5$. We considered a maximum mass ratio 1:3 and assumed a maximum gas fraction of merging galaxies of 0.2. The merger rate per galaxy we derived at $z = 4$ is 0.013 Gyr^{-1} and thus, keeping constant this rate between $1.5 - 2 \lesssim z < 5$, the number of mergers per galaxy in 2.5 Gyr is just 0.03, two orders of magnitude lower than the one needed. Even relaxing the gas-poor hypothesis by increasing the minimum gas fraction up to ~ 60 per cent, we obtain only one merger event in 2.5 Gyr (a merger rate of $\sim 0.4 \text{ Gyr}^{-1}$). Thus, it seems that the minor merger rate predicted by the models is too low to account for the size increase of early compact spheroids needed in the hypothesis that normal ETGs are

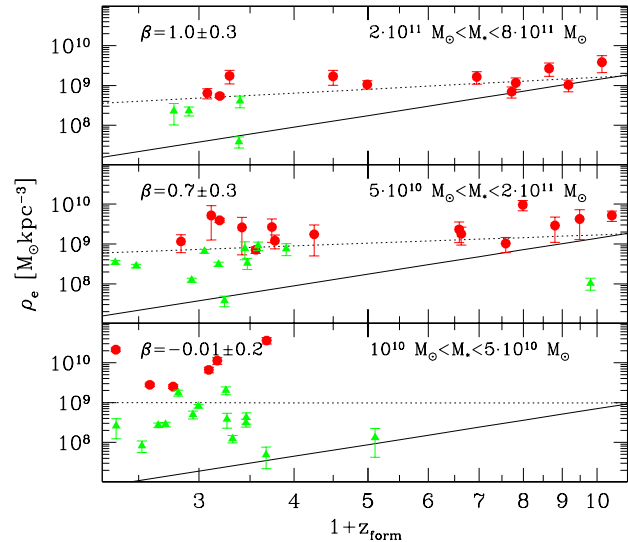


Figure 5. Effective stellar mass density ρ_e as a function of formation redshift z_{form} for ETGs in different ranges of stellar masses. The dotted line represent the best fit to the data obtained by fitting the relation $\rho_e(z_{form}) \propto (1+z_{form})^\beta$. The solid line is the relation $\rho_e(z_{form}) \propto (1+z_{form})^3$ expected in the hypothesis that the higher the redshift of assembly the denser the ETG due to the higher density of the Universe at earlier epochs. The expected relation is normalized to the best fitting value at $z_{form} = 10$. We considered the approximation $z_{assembly} \approx z_{form}$.

their descendants. Our conclusion agrees with the one of Newman et al. (2010) and with the conclusions reached by Tirit et al. (2010) on the basis of different arguments.

Another proposed scheme is that the higher the redshift of assembly the denser the ETG due to the higher density of the Universe at earlier epochs. Since the linear size varies as $(1+z)^{-1}$, in the approximation $z_{assembly} \approx z_{form}$, the effective stellar mass density of a galaxy of fixed mass assembling at different $z_{assembly}$ would scale in this scheme as $\rho_e(z_{assembly}) \approx \rho_e(z_{form}) \propto (1+z_{form})^3$ independently of the mass of the galaxy. In Fig. 5 the effective stellar mass density ρ_e of ETGs in 3 different ranges of stellar masses is shown as a function of their z_{form} . It is interesting to note that the median effective stellar mass density is $\langle \rho_e \rangle \approx 10^9 \text{ M}_\odot \text{ kpc}^{-3}$ in all the three mass ranges. By fitting the data with a scaling relation $\rho_e(z_{form}) \propto (1+z_{form})^\beta$ (dotted line) we obtained $\beta > 0$ in the first two ranges of stellar masses considered ($\beta = 1.0 \pm 0.3$ and $\beta = 0.7 \pm 0.3$ respectively). The significance of these mild correlations is about 90 per cent the Spearman rank test probability being $P_{rs} \gtrsim 0.08$. In Fig. 5 the expected scaling relation $\rho_e(z_{form}) \propto (1+z_{form})^3$ normalized to the value of the best fitting relation at $z_{form} = 10$ is also shown for comparison (solid line). Thus, the correlation between the effective stellar mass density and z_{form} is not so evident from our data as expected in the above scenario. However, we note that z_{form} could not always be a tracer of the assembly epoch, as previously stated, and that the statistics is still low. For these reasons, the lack of the steep scaling relation expected cannot be considered a definite evidence against the above picture.

The results shown in Fig. 4 suggest, at the same time, more naturally the following scheme of formation and assembly. Assuming that dissipative gas-rich merger is the mechanism of spheroids formation, compact ETGs would be a natural consequence of this

mechanism when most of the gas at disposal is burned in the central starburst, as discussed above. To this end, the gas involved in the merger has to be sufficiently cold to collapse toward the center and then ignite the main starburst producing the compact remnant. However, we could suppose that the gas in some of the progenitors is not so cold and homogeneous to allow the rapid central collapse described above and that, consequently, the resulting starburst is not short and intense but much longer and possibly composed of many subsequent starbursts. The rate at which the starburst(s) would be ignited or stoked could be modulated by the cooling time of the different gas clouds composing the gas reservoir and by their orbital and dynamical parameters. In this case the remnant would not be compact and the mean age of the resulting stellar population would be much younger than the one produced in a single and short burst. This qualitative scenario would explain the co-existence of normal and compact ETGs observed at $\langle z \rangle \simeq 1.5$ in spite of the same stellar mass, the lack of normal ETGs with high z_{form} and the absence of any correlation between compactness, stellar mass and formation redshift.

The study of the spatial distribution of the stellar component of ETGs at $z > 1$ can provide fundamental information on their past star formation and assembly histories. The different way in which the stellar population is assembled may produce indeed different colour and light profiles. Such differences should be more pronounced when the stellar populations are young ($< 3 - 4$ Gyr) hence in the high redshift ETGs. For instance, if all the ETGs assemble at high- z ($z_{assembly} > 4 - 5$) as compact/dense spheroids and a fraction of them grow in size by adding a low stellar mass density envelope through dry minor mergers (e.g. Hopkins et al. 2009; Naab et al. 2009) we should observe compact ETGs characterized by a coeval stellar population centrally peaked and normal ETGs characterized by a dense core of old stars and an envelope with flatter shape composed of younger stars. On the contrary, in the scenario we have proposed above where the cooling of the gas modulates the compactness and the mean age of the stellar population of galaxies compact and normal ETGs should be characterized by similar surface brightness profile shape but different colour profiles. Thus, compact and normal ETGs should be characterized by different surface brightness and/or color profiles according to the different spatial distribution and density of the stellar populations accreted at different epochs and through different processes. In this regard, we believe that the study of the color gradient of high- z ETGs (Gargiulo et al. 2010) may represent a powerful probe of the early phases of ETGs formation.

4 THE SFR AND THE NUMBER DENSITY OF COMPACT SPHEROIDS IN THE VERY EARLY UNIVERSE

On the basis of the results discussed above and of the data we have at hand we have tried to put constraints on the number density of compact spheroids assembled in the very early Universe and on the resulting contribution to the SFR density. The compact ETGs with $z_{form} > 5$ have stellar masses $M_* = [1 - 5] \times 10^{11} M_\odot$ (Fig. 4, middle-right panel). Considering a typical stellar mass of about $1 - 2 \times 10^{11} M_\odot$, according to the gas-rich merger scheme, at least 50 per cent of this mass ($\geq 6 \times 10^{10} M_\odot$) should form in about 1 Gyr during the merging at $z_{assembly} > 5$, as derived above. This implies a mean star formation rate associated to the compact remnant (SFR) $\simeq 60 M_\odot \text{ yr}^{-1}$ at $z > 5$. The two progenitors, with masses (gas+stars) $\sim 6 \times 10^{10} M_\odot$ each, cannot have already formed more

than $3 \times 10^{10} M_\odot$ (50 per cent of mass) of stars each at the epoch of the merging. Since they formed these stellar masses before the merging, that is in about 0.5 Gyr, the required mean SFR is $\sim 60 M_\odot \text{ yr}^{-1}$ also in this case. These (relatively low) values agree with those derived for the star-forming galaxies observed at $z > 5$ (e.g. Hickey et al. 2010; Wilkins et al. 2010) and with the detection of massive galaxies ($> 10^{10} M_\odot$) at $z > 6$ with age 200-700 Myr and $SFR \sim 30 M_\odot \text{ yr}^{-1}$ (e.g. Eyles et al. 2005; 2007). The possible (expected) intense phase of star formation (of some hundreds of M_\odot/yr or more) experienced during the dissipative merger would last for very short times. Indeed, in an exponentially declining star formation history with e-folding time $\tau \simeq 0.1$ Gyr, the star formation rate would drop by a factor ~ 3 in 0.1 Gyr and almost by a factor 10 in 0.2 Gyr. Since 1 Gyr is needed to form most of the stars (see Sec. 3.1), the frequency with which we would observe a dissipative merger during the intense star formation phase would be less than 1:10. This agrees with the apparent lack of strong star-bursting galaxies at very high- z and with the SFRs derived for high-mass spheroidal galaxies observed at $z > 2$ (see also Cava et al. 2010 for very recent results).

We also tried to derive a lower limit to the number density of early compact spheroids at $z > 5$ and to their contribution to the star formation rate density at that redshift. Out of the 13 compact ETGs with $z_{form} > 5$, 3 belong to the ACS sample (Saracco et al. 2010) on the GOODS-South field (143 arcmin²) and 5 to the sample of massive ETGs selected on the S2F1 field (150 arcmin²) (Saracco et al. 2005; Longhetti et al. 2007). The co-moving volumes subtended by these two fields in the redshift range $4 < z < 9$, that is within ~ 1 Gyr at $z \simeq 5$ are $1.51 \times 10^6 \text{ Mpc}^3$ and $1.64 \times 10^6 \text{ Mpc}^3$ respectively. Thus, the expected number densities of compact spheroids at $z > 5$ derived by these two small samples are $n = 2 \times 10^{-6} \text{ Mpc}^{-3}$ and $n = 3 \times 10^{-6} \text{ Mpc}^{-3}$, from two times lower than the number density ($n = 4 - 5 \times 10^{-6} \text{ Mpc}^{-3}$) of compact ETGs more massive than $10^{11} M_\odot$ observed at $\langle z \rangle \simeq 1.5$ (Saracco et al. 2010) and at $z = 0$ (Valentinuzzi et al. 2010a) to an order of magnitude lower than the number density of compact quiescent galaxies expected at $z > 2$ (e.g. Wuyts et al. 2009; Bezanson et al. 2009). The contribution to the co-moving stellar mass density of these early compact spheroids is $\sim 6 \times 10^5 M_\odot \text{ Mpc}^{-3}$, to be compared with $2.5 \times 10^6 M_\odot \text{ Mpc}^{-3}$, the lower limit to the co-moving stellar mass density at $z \gtrsim 6$ (Eyles et al. 2007). Finally, their contribution to the star formation rate density (SFRD), averaged over 1 Gyr at $z > 5$, is $SFRD \simeq 6 \times 10^{-4} M_\odot \text{ yr}^{-1} \text{ Mpc}^{-3}$, an order of magnitude lower than the total SFRD density estimated at $z \lesssim 6$ (Bouwens et al. 2006; Stark et al. 2007). Thus, all these quantities are well within those derived from the observations of the very high redshift galaxy population. By the way, these latter observations provide supports in favour of the very early formation of compact spheroids whose contribution in terms of stellar mass and star formation rate densities can be significant.

5 SUMMARY AND CONCLUSIONS

We used a sample of 62 ETGs at $0.9 < z_{spec} < 2$ to probe the star formation history and the mass assembly history of early-type galaxies at $z > 2$. Using the local size-mass relation as reference we confirm the co-existence at $\langle z \rangle \simeq 1.5$ of a large number of normal ETGs having $R_e \simeq R_{e,z=0}$ ($10^7 < \rho_e < 10^9 M_\odot \text{ kpc}^{-3}$) with compact ETGs having $R_e = [0.5 - 0.2] R_{e,z=0}$ ($\rho_e > 10^9 M_\odot \text{ kpc}^{-3}$) in spite of the same stellar mass and redshift. We do not see evidence of a

dependence of the compactness and of the stellar mass density ρ_e of ETGs on their stellar mass.

We derived for each galaxy the formation redshift z_{form} at which most of the stellar mass formed. We find that normal ETGs are all segregated at $z_{form} \lesssim 3$ while compact ETGs are distributed over a much wider range, $2 < z_{form} < 10$, with a significant fraction of them (13 out of 33) at $z_{form} > 5$. Earlier stars, those characterized by $z_{form} > 5$, are assembled in compact, more massive ($M_* > 10^{11} M_\odot$) and hence denser ($\rho_e > 10^9 M_\odot \text{ kpc}^{-3}$) ETGs that is, the older the stellar population the higher the mass of the galaxy but not vice versa. Indeed, we see many ETGs with $z_{form} < 3$ and masses as large as those with $z_{form} > 5$. Thus, it seems that the epoch of formation may play a role in the formation of massive ETGs rather than the mass itself.

We have tried to put the above results in the context of hierarchical models of galaxy formation. In a dissipative merging scheme, the known mechanism able to produce compact remnants, where a large fraction of the stellar mass is produced concurrently with the merging, $z_{assembly} \approx z_{form}$. Consequently, compact ETGs would assemble at $2 < z_{assembly} < 10$ with a significant fraction at $z_{assembly} > 5$, according to the z_{form} values obtained. This implies that dissipative gas-rich mergers can efficiently occur also at low redshift in spite of the fact that it should be more probable at high- z thank to the larger amount of gas at disposal. This suggests that the occurrence of dissipative mergers is also dependent on other parameters besides the gas at disposal. The fact that most of the compact high- z ETGs have a local descendant belonging to the galaxy cluster population suggests that the environment may play a role in tuning or triggering dissipative mergers.

We then probed the general scheme in which normal ETGs at $\langle z \rangle \approx 1.5$ are descendants of compact spheroids assembled at $z_{assembly} > 5$. These latter should grow in size (from 2 to 6 times) through dry minor mergers during the 2.5 Gyr at $1.5 - 2 < z < 5$. Using the merger rate calculator by Hopkins et al. we estimated that the number of dry (gas fraction ≤ 0.2) minor (1:3) mergers expected in a hierarchical model at $1.5 - 2 < z < 5$ is two orders of magnitude lower than the one needed. To reach the number of mergers comparable to the one needed, it must be dropped the dissipation-less requirement (i.e. gas fraction 0.6 at least) and relaxed the minor merger requirements ($> 1 : 3$). However, in this case the size would no longer grow with mass as fast as through dry mergers and consequently more mergers would be needed exceeding those predicted by models, and so on. Thus, the hypothesis that normal ETGs are the descendants of dense early spheroids does not find supports in the current models.

Finally, we do not find evidence supporting a dependence of the compactness of galaxies on their redshift of assembly, a dependence expected in the hypothesis that the compactness of a galaxy is due to the higher density of the Universe at earlier epochs. The correlation between the effective stellar mass density and z_{form} expected in the above scenario does not emerge from our data. However, we remind that z_{form} could not always trace the assembly and that the statistics is still low. Hence, the lack of a correlation cannot be considered a definite evidence against the above picture.

The results we obtained studying the dependence of mass, compactness and stellar mass density of ETGs on their formation redshift suggest a clear scenario of formation and assembly of the stellar mass, assuming that dissipative gas-rich merger is the main mechanism of spheroids formation. Indeed, compact ETGs would be a natural consequence of this mechanism when most of the gas at disposal is burned in the central starburst, that is when the gas is sufficiently cold to collapse toward the center and then ignite the

main starburst. However, if the gas of the progenitors was not sufficiently cold and homogeneous the resulting starburst would not be short and intense but longer and possibly composed of many subsequent episodes. The cooling time of the gas clouds and their orbital parameters could modulate the rate at which the starburst(s) are ignited or stoked. This mechanism would produce a larger and younger remnant than the one produced in the short and intense central starburst case. This qualitative scenario would explain the co-existence of normal and compact ETGs observed at $\langle z \rangle \approx 1.5$ in spite of the same stellar mass, the lack of normal ETGs with high z_{form} and the absence of any correlation between compactness, stellar mass and formation redshift.

What our analysis shows is that the stellar mass of ETGs results from different formation histories and that also the way in which the mass has been assembled to form and to shape them is not unique but follows different assembly histories. This arises the question why an ETG follows an assembly history instead of another one. It is obvious to wonder if the environment plays a role in setting out the formation and the destiny of an ETG. The fact that most of the compact high- z ETGs have a local descendant belonging to the galaxy cluster population suggests that the environment can play a role in accounting for the diversities (see also Rettura et al. 2010). Fundamental insights on the past star formation and assembly histories of ETGs can come from the study of the spatial distribution of their stellar component. In this regard we believe that color gradients represent a promising tool to investigate the past history of high- z ETGs.

ACKNOWLEDGMENTS

This work is based on observations made with the ESO telescopes at the Paranal Observatory and with the NASA/ESA Hubble Space Telescope, obtained from the data archive at the Space Telescope Science Institute which is operated by the Association of Universities for Research in Astronomy. We thank the referee for the constructive comments. We acknowledge financial contribution from the agreements ASI-INAF I/016/07/0 and I/009/10/0.

6 REFERENCES

- Bernardi, M., Hyde, J. B., Fritz, A., Sheth, R. K., Gebhardt, K., Nichol, R. C. A., 2008, MNRAS, 391, 1191
 Bezanson R., van Dokkum P. G., Tal T., Marchesini D., Kriek M., Franx M., Coppi P. 2009, ApJ, 697, 1290
 Bouwens R. J., Illingworth G. D., Blakeslee J., Franx M. 2006, ApJ, 653, 53
 Boylan-Kolchin M., Ma C.-P., Quataert E. 2006, MNRAS, 369, 1089
 Boylan-Kolchin M., Ma C.-P., Quataert E. 2008, MNRAS, 383, 93
 Buitrago F., Trujillo I., Conselice C. J., Bouwens R. J., Dickinson M., Yan H. 2008, ApJ, 687, L61
 Cappellari M., di Serego Alighieri S., Cimatti A., et al. 2009, ApJ, 704, L34
 Carrasco E. R., Conselice C. J., Trujillo I. 2010, MNRAS, 405, 2253
 Cassata P., et al. 2010, ApJ, 714, L79
 Cenarro A. J., Trujillo I. 2009, A&A, 501, 119
 Chabrier G. 2003, PASP, 115, 763
 Cimatti A., et al. 2004, Nat., 430, 184
 Cimatti A., et al. 2008, A&A, 482, 21

- Ciotti L., Lanzoni B., Volonteri M. 2007, *ApJ*, 658, 65
- Cowie L. L., Songaila A., Hu E. M., Cohen J. G. 1996, *AJ*, 112, 839
- Daddi E., Renzini A., Pirzkal N., et al. 2005, *ApJ*, 626, 680
- Damjanov I., McCarthy P. J., Abraham R. G., et al. 2009, *ApJ*, 695, 101
- De Lucia G., Springel V., White S. D. M., Croton D., Kauffmann G. 2006, *MNRAS*, 366, 499
- Dunlop J., Peacock J., Spinrad H., Dey A., Jimenez R., Stern D., Windhorst R. 1996, *Nat.* 381, 581
- Eyles L. P., Bunker A. J., Stanway E. R., Lacy M., Ellis R. S., Doherty M. 2005, *MNRAS*, 364, 443
- Eyles L. P., Bunker A. J., Ellis R. S., Lacy M., Stanway E. R., Stark D. P., Chiu K. 2007, *MNRAS*, 374, 910
- Fukugita M., Hogan C. J., Peebles P. J. E. 1998, *ApJ*, 503, 518
- Gargiulo A., et al., 2009, *MNRAS*, 397, 75
- Gargiulo A., Saracco P., Longhetti M. 2010, *MNRAS* in press [arXiv:1011.2427]
- Gavazzi G., Boselli A., Pedotti P., Gallazzi A., Carrasco L. 2002, *A&A*, 396, 449
- Giavalisco, M., Dickinson, M., Ferguson, H. C., et al. 2004, *ApJ*, 600, L103
- Glazebrook K., et al. 2004, *Nat.* 430, 181
- Hickey S., Bunker A., Jarvis M. J., Chiu K., Bonfield D. 2010, *MNRAS*, 404, 212
- Hopkins, P. F., Cox T. J., Hernquist L. 2008, *ApJ*, 689, 17
- Hopkins, P. F., Bundy, K., Murray N., Quataert E., Lauer T. R., Ma C.-P. 2009, *MNRAS*, 398, 898
- Hopkins, P., et al. 2010b, *ApJ*, 715, 202
- Khochfar S., Silk J. 2006a, *ApJ*, 648, L21
- Khochfar S., Silk J. 2006b, *MNRAS*, 370, 702
- Kurk J., et al., 2009, *A&A*, 504, 331
- La Barbera F., de Carvalho R. R., *ApJ*, 699, L76
- Longhetti M., Saracco P., Severgnini P., et al., 2005, *MNRAS*, 361, 897
- Longhetti M., Saracco P., Severgnini P., et al., 2007, *MNRAS*, 374, 614
- Mancini, C., Daddi E., Renzini A., et al. 2010, *MNRAS*, 401, 933
- McCarthy P. J., et al. 2004, *ApJ*, 614, L9
- McGrath E., Stockton A., Canalizo G., Iye M., Maihara T. 2008, *ApJ*, 682, 303
- Muzzin A., van Dokkum P. G., Franx M., Marchesini D., Kriek M., Labbé I. 2009, *ApJ*, 706, L188
- Naab T., Johansson P. H., Ostriker J. P., Efstathiou G. 2007, *ApJ*, 658, 710
- Naab T., Johansson P. H., Ostriker J. P. 2009, *ApJ*, 699, L178
- Newman A. B., Ellis R. S., Treu T., Bundy K. 2010, *ApJ*, [arXiv:1004.1331]
- Onodera M. et al. 2010, *ApJ*, in press [arXiv:1004.2120]
- Rettura A., et al., 2010, *ApJ*, 709, 512
- Ryan Jr. E. R., et al. 2010, *ApJ* submitted [arXiv:1007.1460]
- Saracco P., Longhetti M., Severgnini P., et al. 2003, *A&A*, 398, 127
- Saracco P., Longhetti M., Severgnini P., et al. 2005, *MNRAS*, 357, L40
- Saracco P., Longhetti M., Andreon S., 2009, *MNRAS*, 392, 718
- Saracco P., Longhetti M., Gargiulo A. 2010, *MNRAS*, 408, L21
- Serra P., Trager S. C. 2007, *MNRAS*, 374, 769
- Shen S., et al., 2003, *MNRAS*, 343, 978
- Sommer-Larsen J., Toft S., 2010, *ApJ*, 721, 1755
- Springel V., Hernquist L. 2005, 622, L9
- Stark D. P., Bunker A. J., Ellis R. S., Eyles L. P., Lacy M. 2007, *ApJ*, 659, 84
- Strazzullo V., et al. 2010, *A&A* in press [arXiv:1009.1423]
- Thomas D., Maraston C., Bender R., Mendes de Oliveira C. 2005, *ApJ*, 621, 673
- Thomas D., Maraston C., Schawinski K., Sarzi M., Silk J. 2010, *MNRAS*, 404, 1775
- Tiret O., Salucci P., Bernardi M., Maraston C., Pforr J. 2010, *MNRAS*, in press [arXiv:1009.5185]
- Trujillo I., Feulner G., Goranova Y., et al. 2006, *MNRAS*, 373, L36
- Trujillo I., Cenarro A. J., de Lorenzo-Cáceres A., Vazdekis A., de la Rosa I. G., Cava A. 2009, *ApJ*, 692, L118
- Valentinuzzi P., et al. 2010a, *ApJ*, 712, 226
- Valentinuzzi P., et al. 2010b, *ApJL*, in press [arXiv:1007.4447]
- van der Wel A., Bell E. F., van den Bosch F. C., Gallazzi A., Rix H. 2009, *ApJ*, 698, 1232
- van Dokkum P. G., et al. 2008, *ApJ*, 677, L5
- van Dokkum P. G., Kriek M., Franx M. 2009, *Nature*, 460, 717
- Wilkins S. M., Bunker A. J., Ellis R. S., Stark D., Stanway E. R., Chiu K., Lorenzoni S., Jarvis M. J. 2010, *MNRAS*, 403, 938
- Wuyts S., et al. 2009, *ApJ* 700, 799